ELSEVIER

Journal of Power Sources 68 (1997) 618–622

JOURNAL OF POWER SOURCES

Electrochemistry of $LiMnO_2$ over an extended potential range

Z.X. Shu, I.J. Davidson *, R.S. McMillan, J.J. Murray

Institute for Chemical Process and Environmental Technology, National Research Council, Ottawa, Ont., K1A 0R6, Canada

Accepted 14 October 1996

Abstract

A kinetic study of potential versus composition was conducted on orthorhombic $LiMnO_2$ over the voltage range of 1.0 to 4.6 V with a variety of electrolyte formulations. The broad potential range enabled studying the electrochemical behaviour of the material over compositions from $LiMnO_2$ to $Li_{0.1}MnO_2$. Substantial differences in the kinetics of the electrochemical processes associated with certain potential ranges were observed. Crown in right of Canada © 1997 Published by Elsevier Science S.A.

Keywords: Lithium batteries; Lithium, Manganese dioxide; Cathodes

1. Introduction

$LiMnO_2$ is known to exist in several phases. Two phases, whose crystal structures have been well characterized, are a tetragonal spinel-related phase, usually written as λ-$Li_2Mn_2O_4$, and an orthorhombic phase. Guyomard and Tarascon [1] have demonstrated that lithium-ion cells with cathodes based on the spinel phase λ-$Li_{2-x}Mn_2O_4$ can have long cycle life at reasonable energy and power densities. More recently, it was found that cathodes made with orthorhombic $LiMnO_2$ undergo a phase transition, on cycling, to form the spinel phase λ-$Li_{2-x}Mn_2O_4$ in situ [2–4]. The orthorhombic form of $LiMnO_2$ has the advantages of being easy to prepare and air stable [2] whereas the spinel phase, λ-$Li_{2-x}Mn_2O_4$, is not air stable at small values of x and is more difficult to make in a fully lithiated form [5]. The use of orthorhombic $LiMnO_2$ in a prototype lithium-ion cell with a coke anode was demonstrated previously [6]. Here, we investigate the kinetics of the electrochemical processes occurring in cathodes based on orthorhombic $LiMnO_2$ in cells with metallic lithium anodes.

2. Experimental

High temperature orthorhombic $LiMnO_2$ was prepared in-house by a procedure described previously [6]. Scanning electron microscopy (SEM) showed that the $LiMnO_2$ particles were layered platelets of varying sizes, typically between 5 and 20 μm. A measurement of the surface area by krypton gas adsorption, using a Micromeritics ASAP 2000, found an area of 0.306(1) m^2/g of $LiMnO_2$. Electrodes were formed by mixing orthorhombic $LiMnO_2$ with carbon black (Super-S, S. Ensagri) and poly(vinylidene fluoride) (PVDF) (301F, Elf Atochem) in a weight ratio of 88:9:3. The cathodes had a diameter of 1.1 cm and a thickness between 0.005 and 0.010 cm. The $LiMnO_2$ electrodes were cycled in NRC designed and fabricated 2325 coin cells having 23 mm diameter and 2.5 mm height and a polypropylene grommet. The anodes were punched from a 5 mm thick sheet of lithium metal (Foote), and had a diameter of 1.65 cm. Two layers of microporous polypropylene (Celgard 3501) were used as the separators. Stainless-steel disc springs (Belleville) and disc spacers were needed to establish enough force on the electrode assemblies (18 kg) to ensure reliable internal contact. Fig. 1 is an exploded view of the cell assembly. The coin cells were assembled and crimp sealed in a dry box filled with helium. All cell cycling was done galvanostatically between voltage limits.

Several electrolytes were used in the electrochemical characterization of orthorhombic $LiMnO_2$. They were 1 M $LiPF_6$ (Hashimoto) in ethylene carbonate (EC, Aldrich)/dimethyl carbonate (DMC) (1/2), 1 M $LiClO_4$ in propylene carbonate (PC, Anachemia)/dimethoxyethane (DME, Anachemia) (1/1), 1 M $LiClO_4$ in EC/diethyl carbonate (DEC, Aldrich) (1/1) and 1 M $LiClO_4$ in PC/EC (1/1). The electrolyte solvents were first dried for 24 h over activated molecular sieves and were then distilled using a spinning band column. In the case of PC and EC, distillations were carried out under vacuum. $LiPF_6$ was used without further purification. $LiClO_4$

* Corresponding author.

0378-7753/97/$17.00 Crown in right of Canada © 1997 Published by Elsevier Science S.A.
PII S0378-7753(96)02571-2

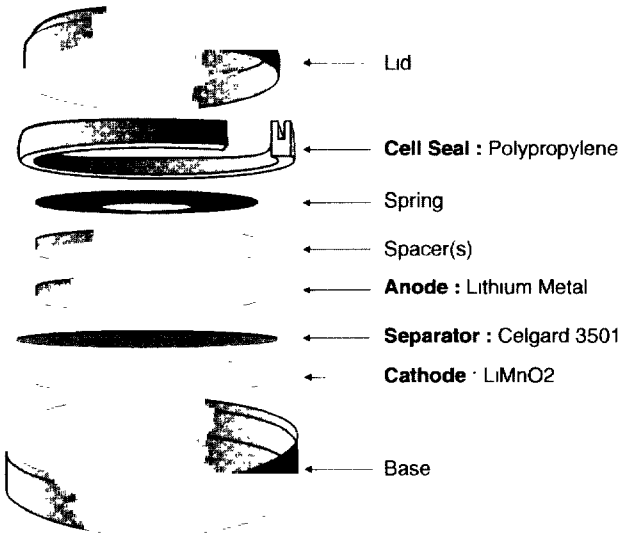

Fig. 1. Exploded view of coin cell assembly used for these studies.

was dried under vacuum at 120 °C overnight. The water contents of the electrolyte solutions were measured using Karl–Fisher titration and were less than 50 ppm.

X-ray powder diffraction (XRD) patterns were obtained on cathodes extracted from previously cycled coin cells. A Scintag XDS 2000 with a θ–θ geometry and a copper X-ray tube was used to obtain the data. The diffractometer has a pyrolytic graphite monochromator in front of the detector. The samples were mounted on a zero background sample holder made from an oriented silicon wafer. The air-sensitive samples were removed from the cells in an argon filled dry box and heat-sealed in a polyethylene bag for the diffraction studies. In some cases, the cathodes could not be removed from the microporous polypropylene separator film. For these diffraction patterns, the second layer of separator from the same cell was used to establish an appropriate background correction which also includes contributions from dried electrolyte. Lattice parameters were calculated from the measured peak positions with the program TREOR [7]. Relative intensities of peaks were obtained by profile fitting to a Pearson VII curve shape. Since the diffraction patterns of ex situ cathodes have very broad peaks, no attempt was made to correct the relative intensities for Lorentz-polarization or absorption.

3. Results and discussion

Lithium-ion cells with coke anodes and a cathode of either orthorhombic $LiMnO_2$ or λ-$Li_{2-x}Mn_2O_4$ have previously been shown to have a first cycle, coulombic inefficiency of 45–80 mAh/g of active material [5,6]. This irreversible loss of capacity was attributed to the formation of a passivation film on the surface of the coke.

Fig. 2 shows voltage profiles of the first cycle for several Li/$LiMnO_2$ cells cycled at different rates in 1 M $LiPF_6$ EC/DMC (1/2) between 2.5 and 4.2 V. The most remarkable

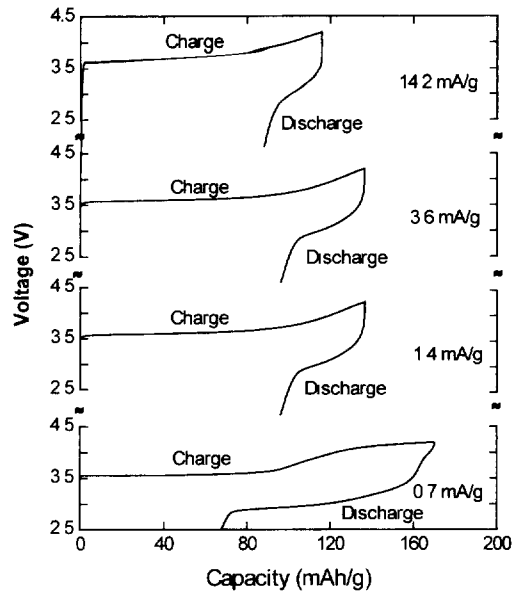

Fig. 2. Voltage profiles of the first cycle for several Li/$LiMnO_2$ cells cycled at different rates in 1 M $LiPF_6$ EC/DMC (1/2) between 2.5 and 4.2 V

feature of these plots is that, even with a lithium anode, there is a large difference in the capacity of the first charge and the first discharge. Both the charge and discharge capacities are very dependent on the current. Constant-rate studies in a coke/$LiMnO_2$ cell showed that the discharge capacity is critically dependent on charging the cell enough to convert the orthorhombic $LiMnO_2$ to spinel $LiMn_2O_4$ [6]. It appears that this phase transition has slow kinetics and the extent of the phase transition during the first cycle is highly dependent on the cycling rate. At a current of 14.2 mA/g of $LiMnO_2$, only a very small amount of orthorhombic $LiMnO_2$ is converted to the spinel phase on the first charge. This is evident from the fact that the charge voltage increases with a steep slope at the cut-off voltage of 4.2 V and the subsequent discharge shows very little reversible capacity from the cell. On the other hand, the cell cycled at 0.7 mA/g shows a clear difference in that the charge voltage curves over to form a plateau before it reaches the cut-off voltage of 4.2 V. In addition, a substantial amount of reversible capacity is obtained on the subsequent discharge. The cells cycled at 3.6 and 1.4 mA/g fall between the two extreme cycling rates mentioned above. At higher currents the phase conversion takes several cycles to complete.

It is not surprising that the kinetics of the phase conversion is slow since it involves a massive rearrangement of the cations in the structure. A detailed mechanism has been proposed by Gummow et al. [4]. The first cycle capacity loss in Li/$LiMnO_2$ cells was somewhat unexpected. The rate dependence of the capacity loss suggests that it is a kinetic rather than a thermodynamic limitation.

After a few cycles in which the spinel phase was formed in situ, some cells were cycled progressively to a higher charge cut-off voltage. Fig. 3 shows typical voltage profiles of an Li/$LiMnO_2$ cell cycled at 3.56 mA/g of $LiMnO_2$ in 1 M $LiPF_6$ in EC/DMC (1/2) to different charge voltage

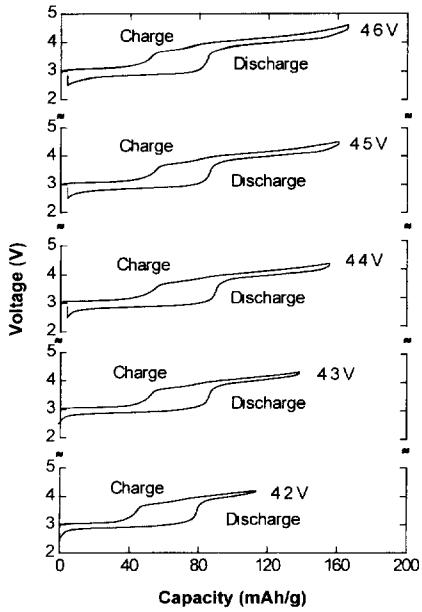

Fig. 3 Voltage profiles of an Li/$LiMnO_2$ cell cycled at 3.56 mA/g of $LiMnO_2$ in 1 M $LiPF_6$ EC/DMC (1/2) between 2.5 V and charge voltage limits from 4.2 to 4.6 V

limits while keeping the discharge cut-off voltage at 2.5 V. The discharge profiles essentially follow the same shape as reported for λ-$Li_2Mn_2O_4$ with a first-order phase transition occurring in the relatively flat lower plateau near 3 V and a homogenous phase transition occurring in the more sloping upper plateau near 4 V [8]. The hysteresis in the voltage profiles is about the same regardless of the voltage limit on charge. Lithium removed from the cathode near 3.8 V, on charge, is re-inserted on discharge in the 2.9 V plateau. The change in slope associated with the hysteresis region of the charge profile suggests that a different crystallographic process is occurring. Not surprisingly, the capacity gain by cycling to a higher voltage mainly occurs at the higher voltage plateau near 4 V. The delithiation of the cathode is almost completely reversible for all voltage limits tested except a small loss of capacity when a cell is charged to a higher voltage presumably due to increased electrolyte decomposition at higher voltage. The charge and discharge capacities of the various cycles are listed in Table 1.

The electrochemical behaviour of $LiMnO_2$ was further investigated at a voltage below 2.5 V after the spinel phase was formed in situ. This was carried out by first charging the cell to 4.2 V in the manner described above, followed by discharging the cell to 1.0 V. Fig. 4 shows voltage profiles of a cell cycled between 4.2 and 1.0 V. Once again, the discharge plateau near 2.9 V is shown to be strongly rate dependent, but the charging hysteresis is independent of rate over the current range studied. In addition, a capacity of about 65 mAh/g is observed between the 2.5–1.0 V range. The discharge capacity below 2.5 V is independent of the cycling rates from 14.2 to 3.6 mA/g and is almost completely reversible. However, this 'extra' capacity between 2.5 and 1.0 V

Table 1
Charge and discharge capacities of Li/$LiMnO_2$ cells cycled at different rates and voltage limits in a variety of electrolytes

Electrolyte (1 M salt)	Voltage (V)	Rate (mA/g)	Charge capacity (mAh/g)	Discharge capacity (mAh/g)
$LiPF_6$ EC/DMC (1/2)	4.2–2.5	3.56	119	113
	4.3–2.5	3.56	138	138
	4.4–2.5	3.56	155	152
	4.5–2.5	3.56	161	157
	4.6–2.5	3.56	165	164
$LiPF_6$ EC/DMC (1/2)	4.2–1.0	3.56	203	199
	4.3–1.0	3.56	214	210
	4.3–1.0	1.78	255	227
	4.4–1.0	3.56	225	220
	4.5–1.0	3.56	235	227
$LiClO_4$ EC/DMC (1/2)	4.4–1.0	3.56	269	257
$LiClO_4$ PC/DME (1/1)	4.2–1.0	1.78	219	208
	4.4–1.0	1.78	248	230
$LiClO_4$ PC/EC (1/1)	4.2–1.0	1.78	228	224
	4.3–1.0	1.78	246	243
	4.4–1.0	1.78	253	250

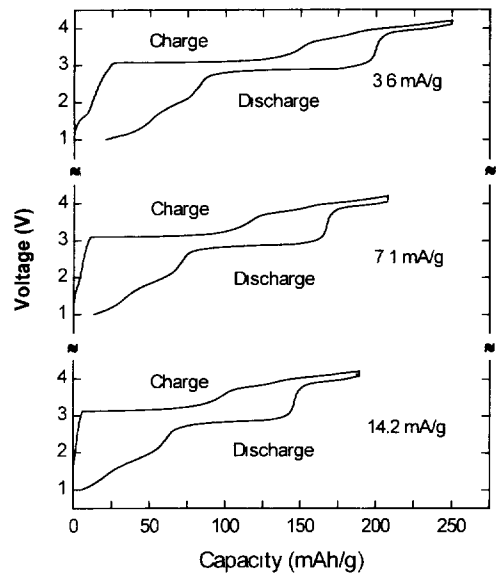

Fig. 4 Voltage profiles of a cell cycled between 1.0 and 4.2 V at various rates.

appears in the recharge at 3.05 V. In fact, cells discharged to 1.0 V and then monitored for voltage changes in the absence of current flow were found to relax to greater than 2.0 V in 3.5 h, and reach a maximum of 2.94 V after about 80 h. Depending on the electrolyte used and the cycling rate, the total reversible capacity between 1.0 and 4.4 V, under our non-optimized conditions, can be as high as 90% of the theoretical capacity of $LiMnO_2$. Table 1 lists charge and discharge capacities for several cells cycled in different electrolytes.

The spinel-related structure of $LiMnO_2$ after the in situ phase transition was confirmed by XRD. This was carried out

Table 2
X-ray diffraction data for cathodes extracted from cycled coin cells after charging to 4.2 V and after discharging to 1.0 V

Cathode at 4.2 V $Li_{0.87}Mn_2O_4$			Cathode at 1.0 V $Li_2Mn_2O_4$		
d (Å)	(hkl)	Relative intensity	d (Å)	(hkl)	Relative intensity
a = 8.174(1) Å	$Fd3m$	Cu Kα	a = 5.658(2) Å c = 9.232(4) Å	$I4_1/amd$	Cu Kα
4.685	111	91	4.8 *	101	40
2.456	311	52	2.691	103	10
2.355	222	14	2.46 *	211	15
2.040	400	100	2.407	202	11
1.875	331	5	2.302	004	10
1.574	511	33	1.999	220	23
1.444	440	72	1.510	224	23
1.381	531	22	1.414	400	7
1.233	622	15	1.350	206	<5
1.179	444	14	1.222	422	<5
1.145	551	<5	1.207	404	6
1.064	553+731	<5	1.154	008	<5
1.022	800	9			

* Peaks marked with an asterisk overlapped with peaks from the separator and are not accurate. These peaks were not used in the calculation of the lattice parameters

by first cycling the cell for a number of cycles and allowing a complete phase transition as indicated by the voltage profile. A cell was then taken apart after charging it to 4.2 V. The cathode was completely extracted from the separator before obtaining the XRD data listed in Table 2. The XRD pattern indexed to a cubic crystallographic unit cell with a lattice parameter of 8.174(1) Å. This corresponds to a composition of $Li_xMn_2O_4$ in which $x = 0.87$ [8]. The relative intensities of the peaks are a reasonable match to the predicted diffraction pattern except that the (111) reflection is weaker than expected. This is most probably due to X-ray absorption which will have the strongest effect on the lowest angle peak.

Two other cells which had been cycled between 4.6 and 1.0 V were disassembled after being discharged to 1.0 V. The cathodes were extracted from the coin cells and sealed in polyethylene bags in an argon-filled glove box. Neither cathode could be removed from the attached separator. The peaks at 4.8 and at 2.46 Å overlapped with peaks associated with the separator and could not be resolved with any accuracy. These peaks were not used in the calculation of the lattice parameters. The XRD patterns of the two cathodes were quite similar. Both patterns indexed to tetragonal cells but the unit cells dimensions were slightly different. The diffraction pattern of the cathode from the first cell refined to lattice parameters of $a = 5.636(4)$ Å and $c = 9.190(6)$ Å, and that of the second cell, to $a = 5.658(2)$ Å and $c = 9.232(4)$ Å. These are comparable with the tetragonal lattice parameters of λ-$Li_2Mn_2O_4$ at $a = 5.646$ Å and $c = 9.250$ Å [8]. The diffraction pattern of the second cathode, listed in Table 2, is a good match to the pattern calculated for λ-$Li_2Mn_2O_4$ on the basis of the structural data in Ref. [8], with the notable exception that the (004) and (224) reflections are much more intense in our diffraction pattern. This may indicate that the crystals of λ-$Li_2Mn_2O_4$ formed in situ in a pressed cathode are not randomly oriented.

4. Conclusions

Orthorhombic $LiMnO_2$ can be cycled over a large composition range (about 90% of its theoretical capacity), but about 25% of this capacity is delivered below 2.5 V versus metallic lithium. In a lithium-ion cell, the $LiMnO_2$ cathode capacity below 2.5 V is a good match to the irreversible capacity needed to passivate the carbon anode. However, improved anode/electrolyte formulations may, in future, lessen the capacity loss due to anode passivation. Therefore, it is important to understand the chemistry of the large voltage hysteresis at the end of discharge of an $LiMnO_2$ cathode. Since the capacity below 2.5 V is not as sensitive to rate as the capacity of the 2.9 V plateau, we propose that the lower voltage capacity is due to the formation of a metastable phase which is richer in lithium than the bulk of the cathode. Over time, normally several hours, the cell voltage rises to 2.9 V as the lithium concentration in the cathode equilibrates to form λ-$Li_{2-x}Mn_2O_4$. The identity of the proposed metastable phase is not yet known, but one possibility is, Li_2MnO_2. This phase has a trigonal crystal structure consisting of hexagonally-close-packed anions with octahedrally coordinated Mn^{2+} ions in alternate basal planes and Li^+ ions in tetrahedral sites of the other basal planes [9]. A similar chemistry occurs in lithium cells with $LiNiO_2$ cathodes in which Li_2NiO_2 is formed on over-discharge [10].

The kinetics of the initial phase transition to the spinel form and of re-insertion of the last 25% or so of the Li^+ ions into the λ-$Li_{2-x}Mn_2O_4$ structure are undesirably slow. In the spinel phase $LiMn_2O_4$, small modifications to the stoichiometry have been shown to have a dramatic affect on the electrochemical performance in the 4 V region [11]. Clearly, similar studies on the orthorhombic phase are warranted. Alternatively, using a slightly higher temperature for the first forming cycle or preparing the material as crystallites of smaller size might improve the kinetics of both the phase conversion and the re-insertion process.

Acknowledgements

The authors wish thank Helen Slegr for technical assistance with moisture analyses, solvent distillation, electrolyte preparation and BET surface area measurement, and Tom Adams for the preparation of $LiMnO_2$. Financial support from the Department of National Defense, Canada, is gratefully acknowledged.

References

[1] D. Guyomard and J.M. Tarascon, *J. Electrochem. Soc., 139* (1992) 937–948.
[2] I.J. Davidson, R.S. McMillan and J.J. Murray, *US Patent No. 5 506 078* (1996).
[3] J.N. Reimers, E.W Fuller, E. Rossen and J.R. Dahn, *J Electrochem. Soc., 140* (1993) 3396–3401
[4] R.J. Gummow, D.C. Liles and M.M. Thackeray, *Mater. Res. Bull., 28* (1993) 1249–1256.
[5] J.M. Tarascon and D. Guyomard, *J. Electrochem. Soc., 138* (1991) 2864–2868.
[6] I.J. Davidson, R.S. McMillan, J.J Murray and J.E. Greedan, *J Power Sources, 54* (1995) 232–235.
[7] P.E. Werner, L Eriksson and M. Westdahl, *J. Appl. Crystallogr., 18* (1985) 367–370.
[8] T Ohzuku, M Kitagawa and T Hirai, *J. Electrochem. Soc., 137* (1990) 769–775.
[9] W.I.F. David, J.B. Goodenough, M.M. Thackeray and M G.S.R. Thomas, *Rev. Chim. Mineral, 20* (1983) 636–642.
[10] J.R. Dahn, U. von Sacken and C.A Michal, *Solid State Ionics, 44* (1990) 87–97.
[11] Y. Guo and J R. Dahn, *J. Electrochem. Soc., 143* (1996) 100–114.